lamps. The temperature of the reactor was maintained at 40 °C by allowing a stream of air to flow through the apparatus during the period of irradiation. Samples (3.0 mL) were placed in quartz tubes (Ace Glass, 170 cm × 15 mm) that were equipped with Pyrex glass sliding stoppers and degassed through 3 or 4 freeze–pump–thaw cycles. The tubes were then sealed in vacuo and irradiated for 30 min. Quantum yields of the photoproducts were determined with cyclopentanone as the actinometer. Acetophenone was used as the sensitizer, and the yields (mol %) of products were determined with dodecane as an internal standard.

Ultraviolet and NMR studies were carried out over a wide range of pentachlorobenzene concentrations to determine if a ground-state charge-transfer complex with triethylamine is formed. There was no evidence for a charge-transfer complex with either spectral technique.

Product Analyses. The photolysis mixtures were analyzed by gas chromatography on a Varian 3700 gas chromatograph equipped with a flame ionization detector. A 6-ft column, 15% Carbowax (20 M) supported on Chromsorb P, AW/DMCS (60/80 mesh), was used. The temperature of the column was programmed from 90 °C for 18 min to 180 °C at 5 deg/min., while the helium gas flow was 30 mL/min; the injector port and the detector temperatures were maintained at 180 and 240 °C, respectively. These conditions were found to be most suitable, especially for resolving the peaks for 1,2,3,5- and 1,2,4,5-tetrachlorobenzenes. Also, of all the stationary phases and supports tried, Carbowax (20 M) and Chromsorb-P proved to be the best choice for this purpose. The photoproducts were identified by comparing their gas chromatographic retention times with those of the known compounds and by mass spectrometry. The MS analyses were carried out on a Finnigan 4023 mass spectrometer equipped with a Finnigan 9610 gas chromatograph.

Acknowledgment. We express our appreciation to the National Institute of Environmental Health Sciences (ES00040) for support of this work.

Registry No. 1,3-DCB, 541-73-1; 1,3-DCB (radical anion), 63697-17-6; 1,4-DCB, 106-46-7; 1,4-DCB (radical anion), 55232-43-4; 1,2-DCB, 95-50-1; 1,2-TCB (radical anion), 34531-00-5; 1,3,5-TCB, 108-70-3; 1,3,5-TCB (radical anion), 63697-19-8; 1,2,4-TCB, 120-82-1; 1,2,4-TCB (radical anion), 63697-18-7; 1,2,3-TCB, 87-61-6; 1,2,3-TCB (radical anion), 51703-47-0; 1,2,3,5-TCB, 634-90-2; 1,2,3,5-TCB (radical anion), 63697-21-2; 1,2,4-TCB, 95-94-3; 1,2,4,5-TCB (radical anion), 63697-22-3; 1,2,3,4-TCB, 634-66-2; 1,2,3,4-TCB (radical anion), 63697-20-1.

A Method of Transition-State Mapping for Arenesulfonate Leaving Groups

Robert V. Hoffman* and Jean M. Shankweiler

Contribution from the Department of Chemistry, New Mexico State University, Las Cruces, New Mexico 88003, *Received December 26, 1985, Revised Manuscript Received May 31, 1986*

Abstract: Equilibrium data for methyl transfer between arenesulfonate groups can be plotted vs. rate data in Brønsted-type plots to give $\beta_{lg}^{CH_3}$. This parameter measures the extent of arenesulfonate loss at the transition state. Its use in transition-state mapping is demonstrated for several elimination and substitution reactions.

The development of methods for characterizing the transition states of organic reactions has been a primary goal of organic chemists for decades. The most simple and perhaps the most informative structural feature of the transition state of a reaction is the extent of bond breaking and/or bond making that has occurred. For multibond reactions the bond making and bond breaking are not necessarily linked, and each can proceed to different extents at the transition state. The relationship between bonding change and the energy of the transition state has been developed by the use of More–O'Ferrall–Jencks (MOFJ) diagrams,[1] which are three-dimensional reaction-coordinate diagrams. Two dimensions are used to express bonding changes that occur during the reaction, and the third is reserved as an energy coordinate.[2] MOFJ diagrams are quite useful as a graphical representation of the transition-state structure, and they are also very useful in predicting changes in transition states which will occur as a result of structural changes that are made in the reactants.[3] Thus MOFJ diagrams have proven to be an important conceptual tool in understanding relationships between reactivity, selectivity, and transition-state structure.[1,4]

The utilization of MOFJ diagrams in describing transition-state structures has largely been qualitative. In order to precisely locate the transition state on the energy surface, parameters are needed to accurately describe chemical bonding at the transition state. These can be plotted as coordinates in the MOFJ diagram, thereby locating the transition-state structure on the energy surface. Many important transition-state probes, such as Hammett ρ and isotope effects (k_H/k_D or others), are not suitable for this purpose. The inherent disadvantage of these parameters is that the upper limits they can take are not well-defined. Thus the boundaries of the energy surface over which the transition state can move are not known. For example, parameters measuring charge buildup are not necessarily related to bond breaking.[5] Kinetic isotope effects are more directly related to bond-breaking processes; however, theoretical models must be used to establish the upper limits. In general, uncertainties in the model calculations cause the maximum values to be uncertain for many heavy-atom isotopes.[6] Furthermore, kinetic deuterium isotope effects are rendered uncertain by contributions of tunnelling.[7]

An attractive and convenient way to quantitate the extent of bonding change at the transition state for proton transfers is to

(1) (a) More-O'Ferrall, R. A. *J. Chem. Soc. B* **1970**, 274. (b) Jencks, W. P. *Chem. Rev.* **1972**, *72*, 705. (c) Jencks, D. A.; Jencks, W. P. *J. Am. Chem. Soc.* **1977**, *99*, 7948.

(2) These changes can be formulated in more than three dimensions; however, they are rarely encountered.

(3) (a) Grunwald, E. *J. Am. Chem. Soc.* **1985**, *107*, 125. (b) An excellent discussion of these diagrams is: Lowry, T. H.; Richardson, K. S. *Mechanism and Theory in Organic Chemistry*; Harper and Row: New York, 1981; pp 199–206.

(4) (a) Harris, J. M.; Shafer, S. G.; Moffatt, J. R.; Becker, A. R. *J. Am. Chem. Soc.* **1979**, *101*, 3295. (b) Harris, J. M.; Paley, M. S.; Prasthofer, T. W. *J. Am. Chem. Soc.* **1981**, *103*, 5915. (c) Young, P. R.; Jencks, W. P. *J. Am. Chem. Soc.* **1979**, *101*, 3288.

(5) (a) Johnson, C. D. *The Hammett Equation*; Cambridge University: Cambridge, 1973; p 152. (b) See, for example: Bernasconi, C. F.; Gandler, J. F. *J. Am. Chem. Soc.* **1979**, *101*, 3295.

(6) (a) Melander, L.; Saunders, W. H., Jr. *Reaction Rates of Isotopic Molecules*; Wiley: New York, 1980; Chapter 9, p 258. (b) Hasan, T.; Sims, L. B.; Fry, A. *J. Am. Chem. Soc.* **1980**, *105*, 3967. (c) Koch, H. F.; McLennan, D. J.; Koch, J. G.; Tumas, W.; Dobson, B.; Koch, N. H. *J. Am. Chem. Soc.* **1983**, *105*, 1930. (d) Keefe, J. R.; Jencks, W. P. *J. Am. Chem. Soc.* **1983**, *105*, 265. (e) Brown, K. C.; Romano, F. J.; Suanders, W. H., Jr. *J. Org. Chem.* **1981**, *46*, 4242.

(7) (a) Reference 6a, p 36. (b) Kresge, A. J. *J. Am. Chem. Soc.* **1980**, *102*, 7779 and references therein.

0002-7863/86/1508-5536$01.50/0

Table I. Observed and Calculated K_{lg} Values for Methyl Transfer from Substituted Arenesulfonates to Benzenesulfonate in Sulfolane at 55 °C[a]

$Y-C_6H_4SO_2OMe$	K_{lg}	pK_{lg}
	Observed	
Y = *p*-OMe	0.21	0.68
Y = *p*-Me	0.35	0.46
Y = H	1.00	0
Y = *p*-Cl	5.99	−0.78
Y = 3,4-Cl_2	68.0	−1.83
	Calculated	
Y = *p*-Br	5.52	−0.74
Y = *m*-CF_3	21.4	−1.33
Y = *m*-NO_2	142.3	−2.15
Y = *p*-NO_2	228.6	−2.36
Y = 3,5-$(CF_3)_2$	392.9	−2.59

[a] Observed data taken from ref 13.

use Brønsted parameters. The proportionality constant that relates the rate and pK_a of the catalyst or substrate varies between 0 and 1 for no, or complete, proton transfer at the transition state.[1,8] While these limits need not hold universally, they have been used widely as acceptable descriptors of bonding change.[9]

The loss of a leaving group from a molecule can be treated similarly. The proportionality between the rate of the loss of the leaving group and the pK_a of the leaving group gives β_{lg}, the extent of leaving-group loss at the transition state. While the validity of this idea has been questioned,[10] recent work indicates that it is not at all unreasonable to observe such correlations,[11] particularly if the leaving groups are similar.[10b,11]

We previously applied this method to gauge the loss of arenesulfonates in some elimination reactions (eq 1).[12] Values of β_{lg} were not restricted to 0–1. In fact for these and other reactions

$$RNH_2 + C_6H_5CH_2NH{-}OSO_2Ar \rightarrow C_6H_5CH{=}NH + RNH_3{}^+ArSO_3{}^- \quad (1)$$

which involve loss of arenesulfonate in the rate-determining step, they range up to nearly 3.[12] As such they are not satisfactory parameters to use in MOFJ diagrams because the upper limits are not defined. These variations indicate that the equilibrium proton acidity of arylsulfonic acids, as measured by pK_a (eq 2), is not a proper model for the kinetic behavior of the same arenesulfonate groups when they ionically cleave from a more complex, complicated molecule (eq 2a).

$$ArSO_3H + H_2O \rightleftharpoons ArSO_3{}^- + H_3O^+ \quad (2)$$

$$R{-}OSO_2Ar \rightarrow [R^{\delta+}\cdots{}^{\delta-}OSO_2Ar]^{\ddagger} \rightarrow R^+ + ArSO_3{}^- \quad (2a)$$

Since arenesulfonate leaving groups are commonly used in many reactions, and since aryl substitution leads to minimal structural change of the leaving group, they constitute an ideal series for use in transition-state mapping. What is needed is an equilibrium reaction which more closely models transition states in which these groups are leaving groups.

Lewis and Hu[13] recently published an elegant study in which they reported the equilibrium constants for methyl transfer between arenesulfonates in sulfolane solution at 55 °C (eq 3). If

$$ArSO_2O{-}CH_3 + {}^-OSO_2C_6H_5 \rightleftharpoons ArSO_2O^- + CH_3{-}OSO_2C_6H_5 \quad (3)$$

$$R{-}OSO_2Ar \rightarrow [R^{\delta+}\cdots{}^{\delta-}OSO_2Ar]^{\ddagger} \rightarrow R^+ + {}^-OSO_2Ar \quad (3a)$$

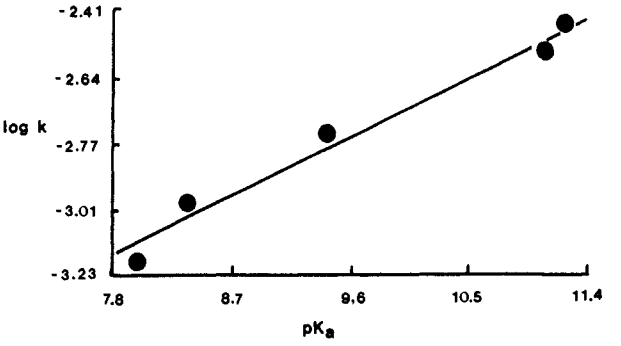

Figure 1. Brønsted plot for proton removal in imine-forming elimination in 2-hexylamine derivative **2**. The rate constants for different promoting bases are plotted vs. the pK_a of each base. The slope is β, and the bases were (left to right in order of ascending rate) *N*-acetylpiperazine, morpholine, tetrahydroisoquinoline, piperidine, and pyrrolidine.

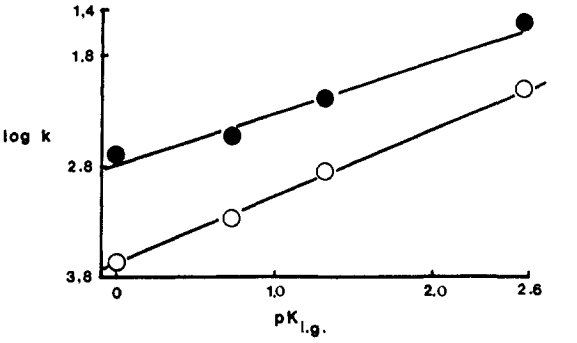

Figure 2. Brønsted plot for leaving-group loss in imine-forming eliminations in (●) *N*-((arylsulfonyl)oxy)benzylamines, **1**, and (○) *N*-((arylsulfonyl)oxy)-2-hexylamines, **2**. Rates are plotted vs. pK_{lg}, and the slopes are $\beta_{lg}{}^{CH_3}$ for these two systems. The (arylsulfonyl)oxy substituents are (left to right in order of increasing rate) H, *p*-Br, *m*-CF_3, and 3,5-$(CF_3)_2$.

benzenesulfonate is chosen as the standard methyl receptor (as water is the reference base in pK_a measurements), then the equilibrium constants K_{lg} for methyl transfer from other arenesulfonates to the reference are shown in Table I. Since benzenesulfonate and methyl benzenesulfonate appear on either side of the equilibrium equation for each different arenesulfonate (eq 3), the equilibrium constants, K_{lg}, are a measure of the free-energy difference between an arenesulfonate bound to a methyl group and the arenesulfonate in its anionic form (in sulfolane solution). This is a much better model for reactions involving the ionization of an arenesulfonate from a complex molecule[14] (eq 3a).

Several arenesulfonate groups of interest were not included in the study by Lewis. Values of K_{lg} for these groups could be calculated, however, from a Hammett plot of Lewis' data (ρ = −2.94; excellent linearity, r = 0.999), and they are included in Table I. With a more suitable model equilibrium defined, the extent of leaving-group loss in the activated complex can be determined by plots of log k vs. pK_{lg} whose slope, $\beta_{lg}{}^{CH_3}$, varies between 0 and 1 for no, or complete, loss of leaving group.

We have applied this method to transition-state mapping of imine-forming eliminations (eq 4). Benzylamine substrate **1** and 2-hexylamine substrate **2**[15] (Ar = *m*-CF_3Ph) were treated with a series of cyclic, secondary amine bases, and the rate of elimination was monitored conductometrically.[16] Plots of log k vs.

$$R_1R_2CH{-}NHOSO_2Ar + B \rightarrow R_1R_2C{=}NH + BH^+{}^-O_3SAr \quad (4)$$

1, $R_1 = C_6H_5$, $R_2 = H$
2, $R_1 = C_4H_9$, $R_2 = CH_3$

pK_a of the base gave β, the extent of proton removal. Figure 1

(8) (a) Gandler, J. R.; Yokoyama, T. *J. Am. Chem. Soc.* **1984**, *106*, 130. (b) Sayer, J. M.; Jencks, W. P. *J. Am. Chem. Soc.* **1977**, *99*, 464. (c) Jencks, W. P. *Acc. Chem. Res.* **1980**, *13*, 161.
(9) (a) Gandler, J. R.; Jencks, W. P. *J. Am. Chem. Soc.* **1982**, *104*, 1937. (b) Saunders, W. H., Jr.; Cockerill, A. F. *Mechanisms of Elimination Reactions*; Wiley: New York, 1973; pp 95–98. (c) For a differing view, see: Pross, A. *J. Org. Chem.* **1984**, *49*, 1811.
(10) (a) Stirling, C. J. M. *Chem. Rev.* **1978**, *78*, 517. (b) Stirling, C. J. M. *Acc. Chem. Res.* **1979**, *12*, 198.
(11) Boyd, D. B. *J. Org. Chem.* **1985**, *50*, 885.
(12) Hoffman, R. V.; Belfoure, E. L. *J. Am. Chem. Soc.* **1982**, *104*, 2183.
(13) Lewis, E. S.; Hu, D. D. *J. Am. Chem. Soc.* **1984**, *106*, 3292.
(14) Williams, A. *Acc. Chem. Res.* **1984**, *17*, 425.
(15) (a) Hoffman, R. V.; Cadena, R. *J. Am. Chem. Soc.* **1977**, *99*, 8226. (b) Hoffman, R. V.; Belfoure, E. L. *Synthesis* **1983**, 34.
(16) Hoffman, R. V.; Belfoure, E. L. *J. Am. Chem. Soc.* **1979**, *101*, 5687.

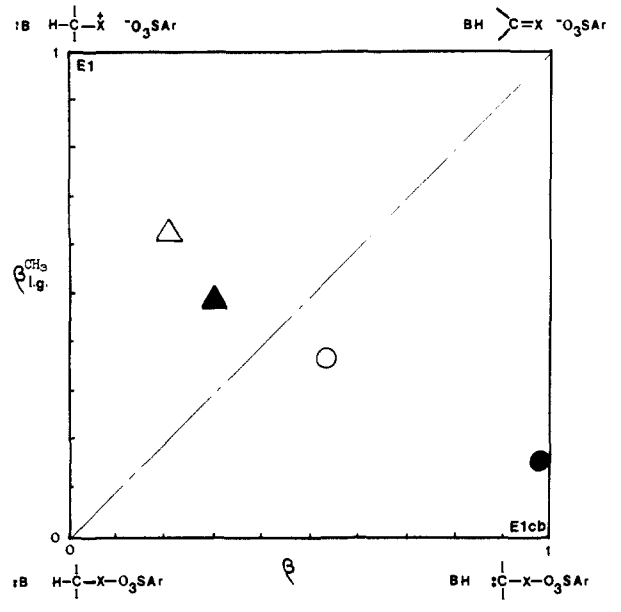

Figure 3. More–O'Ferrall–Jencks (MOFJ) diagram for elimination reactions in which X can be NH for imine-forming eliminations or CH_n for olefin-forming eliminations. Transition-state parameters β and $\beta_{lg}^{CH_3}$ relate to the extent of proton removal and leaving-group loss, respectively, at the transition state. △ is for imine-forming elimination in 2-hexylamine derivative **2**, while ▲ is for benzylamine derivative **1**. ○ is for olefin-forming elimination in 2-phenylethyl arenesulfonates, while ● is for E1cb elimination in 1-(tolylsulfonyl)-2-cyclohexyl arenesulfonates.

shows the results for **2** which gave $\beta = 0.22$ ($r = 0.985$). A value of $\beta = 0.30$ for **1** was determined earlier.[12] Then several arenesulfonate leaving groups were used with morpholine as the promoting base. Plots of log k vs. pK_{lg} (Figure 2) gave $\beta_{lg}^{CH_3}$ for loss of the leaving group.[17] From these plots $\beta_{lg}^{CH_3} = 0.48$ ($r = 0.989$) for **1** and $\beta_{lg}^{CH_3} = 0.62$ ($r = 0.999$) for **2**. These parameters were plotted in the MOFJ diagram in Figure 3. The data illustrate that electron-donating substituents on the α-carbon lead to a more E1-like transition state. Replacement of these by phenyl causes a change in the transition-state structure to a more concerted one.

Olefin-forming eliminations can be treated similarly. Thus for substituted phenylethyl arenesulfonates (eq 5), $\beta_{lg}^{CH_3}$ is found to be 0.41, 0.36, and 0.31 for Z = *p*-CH_3, H, and *m*-Cl, respectively.[18]

$$Z\text{—}C_6H_4CH_2CH_2\text{—}OSO_2Ar + t\text{-}BuO^- \rightarrow \underset{Z = CH_3,\ H,\ Cl}{} Z\text{—}C_6H_4CH{=}CH_2 \quad (5)$$

Here again it is seen that $\beta_{lg}^{CH_3}$ decreases as substituents are more electron withdrawing. Data for the determination of β are not available for these arenesulfonate substrates, but a value of $\beta = 0.54$ has been reported for phenylethyl bromide.[19] Plotting these data in Figure 1 shows these eliminations to be much more E1cb-like. True E1cb reactions have $\beta_{lg}^{CH_3} = 0.15$ (Figure 3).[20] The data dramatically show the transition-state change as a function of structure both within a reaction series and between different reactions.

Another important reaction type is substitution. Irrespective of whether the process is S_N1 or S_N2, an arenesulfonate leaving group is lost ionically in the rate-determining step, and this can be monitored by $\beta_{lg}^{CH_3}$. Leaving-group rate data for several substitutions have been plotted to give $\beta_{lg}^{CH_3}$ and are collected in Table II. Only studies carried out in ethanol are included,

(17) The solvent for all of these studies was an aqueous THF mixture.[15]
(18) Banger, J.; Cockerill, A. F.; Davis, G. L. O. *J. Chem. Soc. B* **1971**, 498.
(19) Hudson, R. F.; Klopman, G. *J. Chem. Soc.* **1964**, 5.
(20) Bordwell, F. G.; Weinstock, J.; Sullivan, T. F. *J. Am. Chem. Soc.* **1971**, *93*, 4728.
(21) Robertson, R. E. *Can. J. Chem.* **1953**, *31*, 589.
(22) Roberts, D. D. *J. Org. Chem.* **1972**, *37*, 1510.

Table II. Arenesulfonate (O_3SAr) Loss in Substitution Reactions in Ethanol as Measured by $\beta_{lg}^{CH_3}$

entry	substrate	type	nucleophile	$\beta_{lg}^{CH_3}$ (r)	ref
1	Me–O_3SAr	S_N2	EtOH	0.45 (0.996)	21
2	Et–O_3SAr	S_N2	EtOH	0.44 (0.992)	21
3	Et–O_3SAr	S_N2	EtO^-	0.47 (0.998)	24
4	1-adamantyl–O_3SAr	S_N1	EtOH	0.60 (0.993)	23
5	2-adamantyl–O_3SAr	S_N1	EtOH	0.61 (0.994)	23
6	*i*-Pr–O_3SAr	S_N1, S_N2	EtOH	0.49 (0.995)	21
7	allyl–O_3SAr	π-assisted	EtOH	0.51 (0.992)	25
8	cyclobutyl–O_3SAr	σ-assisted	EtOH	0.57 (0.996)	22

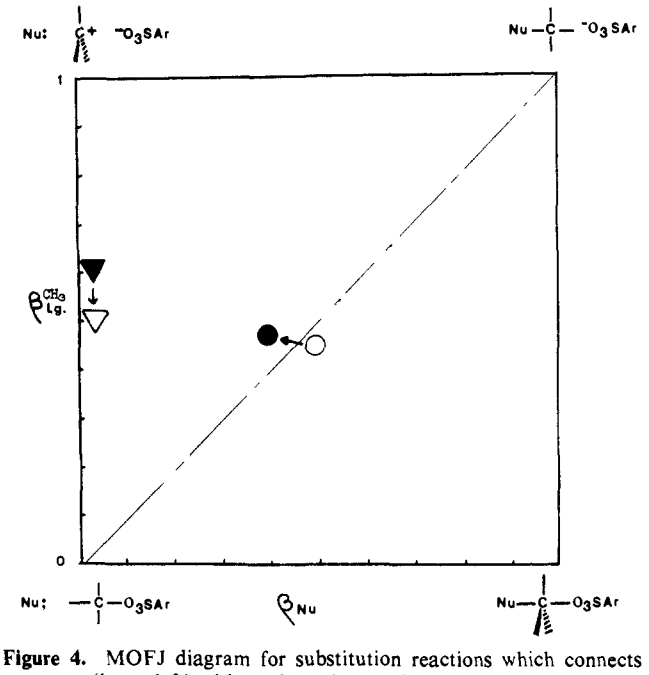

Figure 4. MOFJ diagram for substitution reactions which connects reactants (lower left) with products (upper right). Transition-state parameters β_{Nu} and $\beta_{lg}^{CH_3}$ relate to addition of nucleophile and loss of leaving group, respectively, at the transition state. ○ is for an S_N2 reaction of ethyl arenesulfonates with ethanol as nucleophile, and ● is for ethoxide as nucleophile (β_{Nu} parameters are arbitrary). ▲ is for an S_N1 reaction of 2-adamantyl arenesulfonates, while △ is for an assisted S_N1 process.

to negate solvent influences. The data show that primary substrates which solvolyze by an S_N2 mechanism (Table II, entries 1 and 2) have $\beta_{lg}^{CH_3}$ values of around 0.44. Changing to a more powerful ethoxide nucleophile (entry 3) causes an *increase* in the extent of leaving-group loss in the activated complex, $\beta_{lg}^{CH_3} = 0.47$. While this change in structure of the activated complex is not large, it is real.

The difference in these two systems is a proton. When ethanol is the nucleophile, the activated complex is electron deficient due to the proton on ethanol, **3**. When ethoxide is the nucleophile,

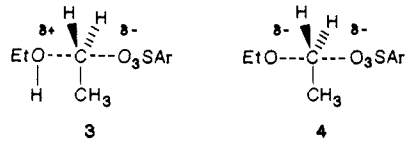

3 **4**

the activated complex is electron rich due to the anionic ethoxide, **4**. Considering the energy surface for substitution (Figure 4), it is seen that the negative charge destabilizes the pentacoordinate intermediate (lower right), causing a shift in structure in the direction of greater leaving-group loss (upper left) and hence larger $\beta_{lg}^{CH_3}$.

Those systems which solvolyze by an S_N1 pathway show much greater leaving-group loss at the transition state (Table II, entries

Table III. Arenesulfonate (O_3SAr) Leaving-Group Loss for Solvolysis of Cyclobutyl Arenesulfonates in Several Solvents[21]

entry	solvent	temp, °C	$\beta_{lg}^{CH_3}$ (r)
1	EtOH	40	0.57 (0.994)
2	AcOH	40	0.49 (0.998)
3	TFE[a]	25	0.45 (0.999)

[a] 2,2,2-Trifluoroethanol.

4 and 5). For these cases, lack of nucleophilic solvation is reflected in higher $\beta_{lg}^{CH_3}$ values of around 0,6. The transition state lies on the left vertical boundary of the energy surface of Figure 4. Surprisingly, the extent of leaving-group loss is only marginally greater for the secondary system than for the tertiary one.

When the loss of the leaving group is facilitated by electron donation to the developing cationic center, then lower $\beta_{lg}^{CH_3}$ values result. The $\beta_{lg}^{CH_3}$ values thus obtained can detect charge-stabilizing events like backside solvation (Table II, entry 6), π-participation (Table II, entry 7), and anchimeric assistance (Table II, entry 8)—all points of current interest.

This technique might also be used to evaluate how solvents affect the structure of the activated complex. The methyl-transfer equilibria (eq 3) used as the basis for determining $\beta_{lg}^{CH_3}$ were determined in sulfolane. This dipolar aprotic solvent is not expected to solvate the arenesulfonate anion well, as indicated by the rather large ρ-value of −2.94 for pK_{lg}.[13] However, since each side of the equilibrium equation has an arenesulfonate anion, and since the solvation of different arenesulfonates is thought to be comparable in a given solvent system,[23] then it is reasonable to expect that the equilibrium constants for methyl transfer should not vary greatly in different solvents since the net free-energy difference between the two sides of eq 3 is due to the electronic character of the arenesulfonate ions. If so, then $\beta_{lg}^{CH_3}$ values for a reaction determined in different solvents reflect the extent of leaving-group loss in each solvent and thus serve to illustrate how the solvent changes the transition state.

We applied this technique earlier to imine-forming eliminations and showed that the activated complex is profoundly influenced by the solvent.[12] Literature data suitable for comparison of many reactions are not common, but Table III indicates that the loss of leaving group in cyclobutyl arenesulfonates varies noticeably with solvent. More-polar solvents cause a decreased amount of leaving-group loss at the transition state. This is in accord with the ability of more-polar solvents to stabilize ionic products (upper left of Figure 4) and cause a parallel shift to an earlier transition state. Solvent effects need more systematic study in order to confirm these arguments.

The method developed here for transition-state mapping can be used in a variety of systems to accurately determine the extent of leaving-group loss in the activated complex. It may therefore prove to be a very useful mechanistic tool.

Acknowledgment. We thank the National Science Foundation (CHE-83-04000) for support of this work.

Registry No. p-$BrC_6H_4SO_2OMe$, 6213-85-0; m-$CF_3C_6H_4SO_2OMe$, 103439-12-9; m-$NO_2C_6H_4SO_2OMe$, 6214-21-7; p-$NO_2C_6H_4SO_2OMe$, 6214-20-6; 3,5-$(CF_3)_2C_6H_3SO_2OMe$, 103439-13-0.

(23) Kevill, D. N.; Kolwyck, K. C.; Shold, D. M.; Kim, C.-B. *J. Am. Chem. Soc.* **1973**, *95*, 6022.

(24) Morgan, M. S.; Cretcher, L. H. *J. Am. Chem. Soc.* **1948**, *70*, 375.

(25) Kevill, D. N.; Rissman, T. J. *J. Org. Chem.* **1985**, *50*, 3062.

True and False Chirality and Absolute Asymmetric Synthesis

L. D. Barron

Contribution from the Chemistry Department, The University, Glasgow G12 8QQ, United Kingdom. *Received November 12, 1985*

Abstract: The concept of true and false chirality is shown to provide a useful criterion for assessing physical systems proposed as agents for inducing absolute asymmetric synthesis. For example, false chirality is exhibited by colinear electric and magnetic fields, true chirality by a magnetic field parallel to the propagation direction of a light beam of arbitrary polarization. General arguments are presented which indicate that only a truly chiral influence can induce absolute asymmetric synthesis in a reaction mixture at thermodynamic equilibrium, but that true chirality is not necessarily required if equilibrium is not attained.

Absolute asymmetric synthesis refers to the use of an external physical influence to produce an enantiomeric excess in what would otherwise be a racemic product of a prochiral chemical reaction.[1] The subject still attracts much interest and controversy[2] and is also central to the problem of the origin of optical activity in nature.[3] One source of confusion is that there are physical systems which can exist in two distinct mirror-image states and yet are not truly chiral in the fundamental sense described later.

A finite cylindrical helix provides a good example of figures exhibiting what Pasteur[4] called *dissymmetry* if they possess structural forms which "differ only as an image in a mirror differs from the object which produces it". Pasteur's extension of the concept of dissymmetry to other aspects of the physical world[5,6] have had a considerable influence on attempts to induce absolute asymmetic synthesis. For example, he held that the combination of a rotation with a linear motion was expected to generate dissymmetry. And since optical rotation can be induced in any sample by a static magnetic field parallel to the light beam (the Faraday effect), he though that a magnetic field was also a source of dissymmetry. Pasteur also sensed a deep cosmic dissymmetry and so anticipated the modern discovery of parity violation in the weak interactions.[7]

Lord Kelvin[8] coined the work *chirality* as an attribute of a geometrical figure "if its image in a plane mirror, ideally realized, cannot be brought to coincide with itself", and this word has now

(1) Morrison J. D.; Mosher, H. S. *Asymmetric Organic Reactions*; American Chemical Society: Washington, DC, 1976.
(2) Mason, S. F. *Int. Rev. Phys. Chem.* **1983**, *3*, 217.
(3) Mason, S. F. *Nature (London)* **1984**, *311*, 19.
(4) Pasteur, L. *Ann. Chim.* **1848**, *24*, 457.
(5) Pasteur, L. *Rev. Scientifique* **1884**, *7*, 2.
(6) Mason, S. F. *Molecular Optical Activity and the Chiral Discriminations*; Cambridge: Cambridge, 1982.
(7) Haldane, J. B. S. *Nature (London)* **1960**, *185*, 87.
(8) Lord Kelvin. *Baltimore Lectures*; C. J. Clay and Sons: London, 1904; p 619.

0002-7863/86/1508-5539$01.50/0